

RESEARCH ARTICLE

Efficacy of a Cell-Cycle Decoying Killer Adenovirus on 3-D Gelfoam[®]-Histoculture and Tumor-Sphere Models of Chemo-Resistant Stomach Carcinomatosis Visualized by FUCCI Imaging

Shuya Yano^{1,2,3}, Kiyoto Takehara^{1,2,3}, Hiroshi Tazawa⁴, Hiroyuki Kishimoto³, Yasuo Urata⁵, Shunsuke Kagawa³, Toshiyoshi Fujiwara^{3,4}, Robert M. Hoffman^{1,2*}

1 AntiCancer, Inc., San Diego, California, United States of America, **2** Department of Surgery, University of California San Diego, San Diego, California, United States of America, **3** Department of Gastroenterological Surgery, Okayama University, Graduate School of Medicine, Dentistry and Pharmaceutical Sciences, Okayama, Japan, **4** Center for Innovative Clinical Medicine, Okayama University Hospital, Okayama, Japan, **5** Oncolys BioPharm Inc., Tokyo, Japan

* all@anticancer.com



OPEN ACCESS

Citation: Yano S, Takehara K, Tazawa H, Kishimoto H, Urata Y, Kagawa S, et al. (2016) Efficacy of a Cell-Cycle Decoying Killer Adenovirus on 3-D Gelfoam[®]-Histoculture and Tumor-Sphere Models of Chemo-Resistant Stomach Carcinomatosis Visualized by FUCCI Imaging. PLoS ONE 11(9): e0162991. doi:10.1371/journal.pone.0162991

Editor: Swati Palit Deb, Virginia Commonwealth University, UNITED STATES

Received: April 13, 2016

Accepted: August 30, 2016

Published: September 27, 2016

Copyright: © 2016 Yano et al. This is an open access article distributed under the terms of the [Creative Commons Attribution License](https://creativecommons.org/licenses/by/4.0/), which permits unrestricted use, distribution, and reproduction in any medium, provided the original author and source are credited.

Data Availability Statement: All data underlying the findings in our study are freely available in the manuscript.

Funding: This study was supported in part by the National Cancer Institute grant CA 132971 and CA142669. This study was also supported in part by grants from the Ministry of Health, Labour, and Welfare, Japan (to T. Fujiwara; No. 10103827, No. 13801426, No. 14525167) and grants from the Ministry of Education, Culture, Sports, Science and Technology, Japan (to T. Fujiwara; No. 25293283).

Abstract

Stomach cancer carcinomatosis peritonitis (SCCP) is a recalcitrant disease. The goal of the present study was to establish an in vitro-in vivo-like imageable model of SCCP to develop cell-cycle-based therapeutics of SCCP. We established 3-D Gelfoam[®] histoculture and tumor-sphere models of SCCP. FUCCI-expressing MKN-45 stomach cancer cells were transferred to express the fluorescence ubiquitinated cell-cycle indicator (FUCCI). FUCCI-expressing MKN-45 cells formed spheres on agarose or on Gelfoam[®] grew into tumor-like structures with G₀/G₁ cancer cells in the center and S/G₂ cancer cells located in the surface as indicated by FUCCI imaging when the cells fluoresced red or green, respectively. We treated FUCCI-expressing cancer cells forming SCCP tumors in Gelfoam[®] histoculture with OBP-301, cisplatin (CDDP), or paclitaxel. CDDP or paclitaxel killed only cycling cancer cells and were ineffective against G₁/G₂ MKN-45 cells in tumors growing on Gelfoam[®]. In contrast, the telomerase-dependent adenovirus OBP-301 decoyed the MKN-45 cells in tumors on Gelfoam[®] to cycle from G₀/G₁ phase to S/G₂ phase and reduced their viability. CDDP- or paclitaxel-treated MKN-45 tumors remained quiescent and did not change in size. In contrast, OB-301 reduced the size of the MKN-45 tumors on Gelfoam[®]. We examined the cell cycle-related proteins using Western blotting. CDDP increased the expression of p53 and p21 indicating cell cycle arrest. In contrast, OBP-301 decreased the expression of p53 and p21. Furthermore, OBP-301 increased the expression of E2F and pAkt as further indication of cell cycle decoy. This 3-D Gelfoam[®] histoculture and FUCCI imaging are powerful tools to discover effective therapy of SCCP such as OBP-301.

The funders had no role in study design, data collection and analysis, decision to publish, or preparation of the manuscript. The funders provided support in the form of salaries for authors [YU], but did not have any additional role in the study design, data collection and analysis, decision to publish, or preparation of the manuscript. The specific roles of all the authors are articulated in the 'author contributions' section.

Competing Interests: We have the following interests: Shuya Yano, Kiyoto Takehara and Robert M. Hoffman are unpaid affiliates of AntiCancer Inc. Hiroyuki Kishimoto was a former affiliates of AntiCancer Inc. Robert M. Hoffman is a PLOS ONE Editorial Board Member. AntiCancer Inc. markets animal models of cancer. Yasuo Urata is President & CEO of Oncolys BioPharma, Inc., the manufacturer of OBP-401. Toshiyoshi Fujiwara is a consultant of Oncolys BioPharma, Inc. H. Tazawa is a consultant of Oncolys BioPharma, Inc. There are no other competing interests. There are no patents, products in development or marketed products to declare. This does not alter our adherence to all the PLOS ONE policies on sharing data and materials. This does not alter our adherence to PLOS ONE policies on sharing data and materials. The specific roles of these authors are articulated in the 'author contributions' section.

Abbreviations: FUCCI, fluorescence, ubiquitination-based cell cycle indicator.

Introduction

Collagen sponge-gel histoculture was developed by Leighton [1] and enables cultured cells to form 3-dimensional structures [2].

As described in detail previously [2], osteosarcoma growing on Gelfoam[®], formed three-dimensional tissue-like structures, but did not form structures in monolayer culture and only colonies on Matrigel[™] [2,3].

As also previously described in detail [3–11], Gelfoam[®] can be used for tumor growth [4, 5], to culture differentiating stem cells [6–8], to culture hair-producing hair follicles [9], to culture hair-growing skin [10] and to culture functional lymphoid tissue [11].

We recently observed that cancer cells in G₀/G₁ phase in Gelfoam[®] histoculture had more extensive migration than in S/G₂/M. Upon entry into S/G₂/M, the cells ceased migrating. After mitosis, when the cells entered G₀/G₁, the cells could resume migrating. The migrating cells in G₀/G₁ were not sensitive to chemotherapy. Fluorescence ubiquitination cell cycle indicator (FUCCI) enabled monitoring of the cell cycle phase of each cell in real time as described in detail previously [12, 13].

We previously showed with FUCCI imaging that cancer cells in Gelfoam[®] and in tumors in mice had a similar cell-cycle-phase distribution. Only the surface cells in Gelfoam[®] histoculture and tumors was cycling; interior cells of tumors and Gelfoam[®] histocultures were quiescent in G₀/G₁. In mono-layer culture, in contrast, cancer cells continuously cycle. In both Gelfoam[®] histoculture and tumors in mice, chemotherapy had similar efficacy, in contrast to cancer cells in mono-layer, which were much more chemo-sensitive as described previously in detail [13–15].

In the present report, we determined the efficacy of cell-cycle decoying telomerase-dependent adenovirus OBP-301 on stomach cancer carcinoma growing on Gelfoam[®] histoculture, using FUCCI imaging to monitor cell-cycle changes.

Materials and Methods

Cells

MKN-45 cells (Cat. #JCRB 0254; Japanese Collection of Research Bioresources, Osaka, Japan), expressing FUCCI, were cultured on plastic plates in RPMI-1640 medium to produce sufficient numbers of cells for Gelfoam[®] histoculture (please see below) [12, 14, 16, 17].

Gelfoam[®] Histoculture

Gelfoam[®] (Pharmacia & Upjohn, Kalamazoo, MI), was cut into 1 cm cubes and placed in 6-well tissue culture plates containing RPMI-1640 medium and placed in a 37°C incubator until the Gelfoam[®] absorbed the medium. FUCCI-expressing cancer cells (1×10⁶) were then carefully layered on top of the Gelfoam[®] and placed in an incubator for 1 h, after which additional medium was added up to the top of the Gelfoam[®] and then incubated again at 37°C with 5% CO₂/95% air, as described previously in detail [2, 4–6, 12, 18].

Establishment of FUCCI-Expressing MKN-45 Cells

In order to establish FUCCI-expressing MKN-45 cells, two plasmids were utilized: mKO2-hCdt1 containing an orange-red fluorescent protein and mAG-hGem, containing a green fluorescent protein (Medical and Biological Laboratory, Nagoya, Japan) [19] were sequentially transfected into MKN-45 cells with the use of Lipofectamine[™] LTX (Invitrogen, Carlsbad, CA). After transfection with each plasmid, the cells were cultured for appropriate

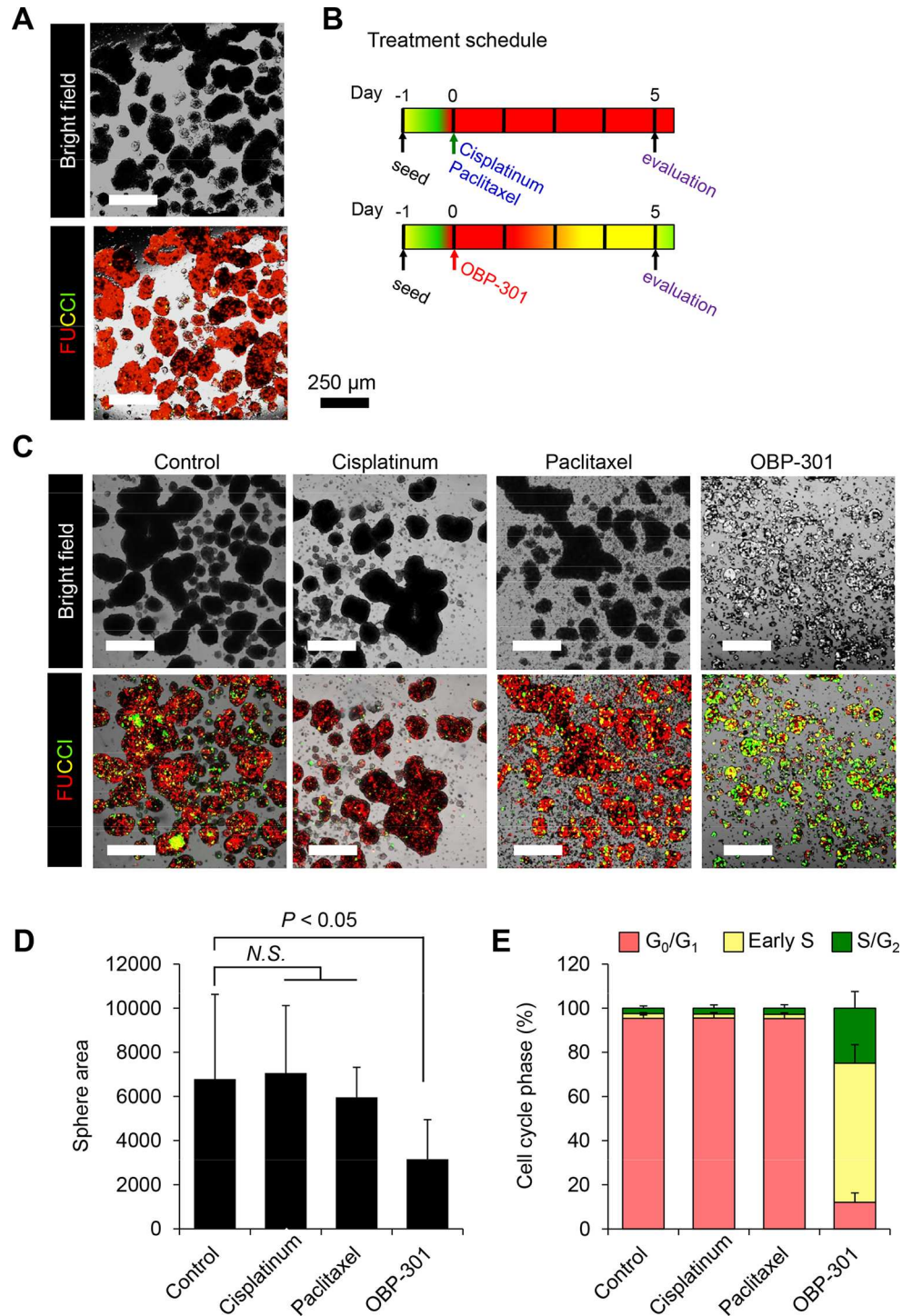


Fig 1. OBP-301 decoys MKN-45 stomach cancer cells in G_1/G_0 to cycle in tumor spheres. A. Representative of FUCCI MKN-45 stomach cancer cells *in vitro*. **B.** Experimental setup for treatment of FUCCI-expressing MKN-45 cells in spheres with OBP-301, cisplatin (CDDP), or paclitaxel. **C.** Representative images of control, OBP-301-, CDDP- or paclitaxel-treated spheres. **D.** Bar graphs show the size of viable tumor spheres after each treatment. **E.** Histogram shows cell cycle phase of treated tumor spheres. Data are shown as means \pm SD ($n = 5$). * $P < 0.01$.

doi:10.1371/journal.pone.0162991.g001

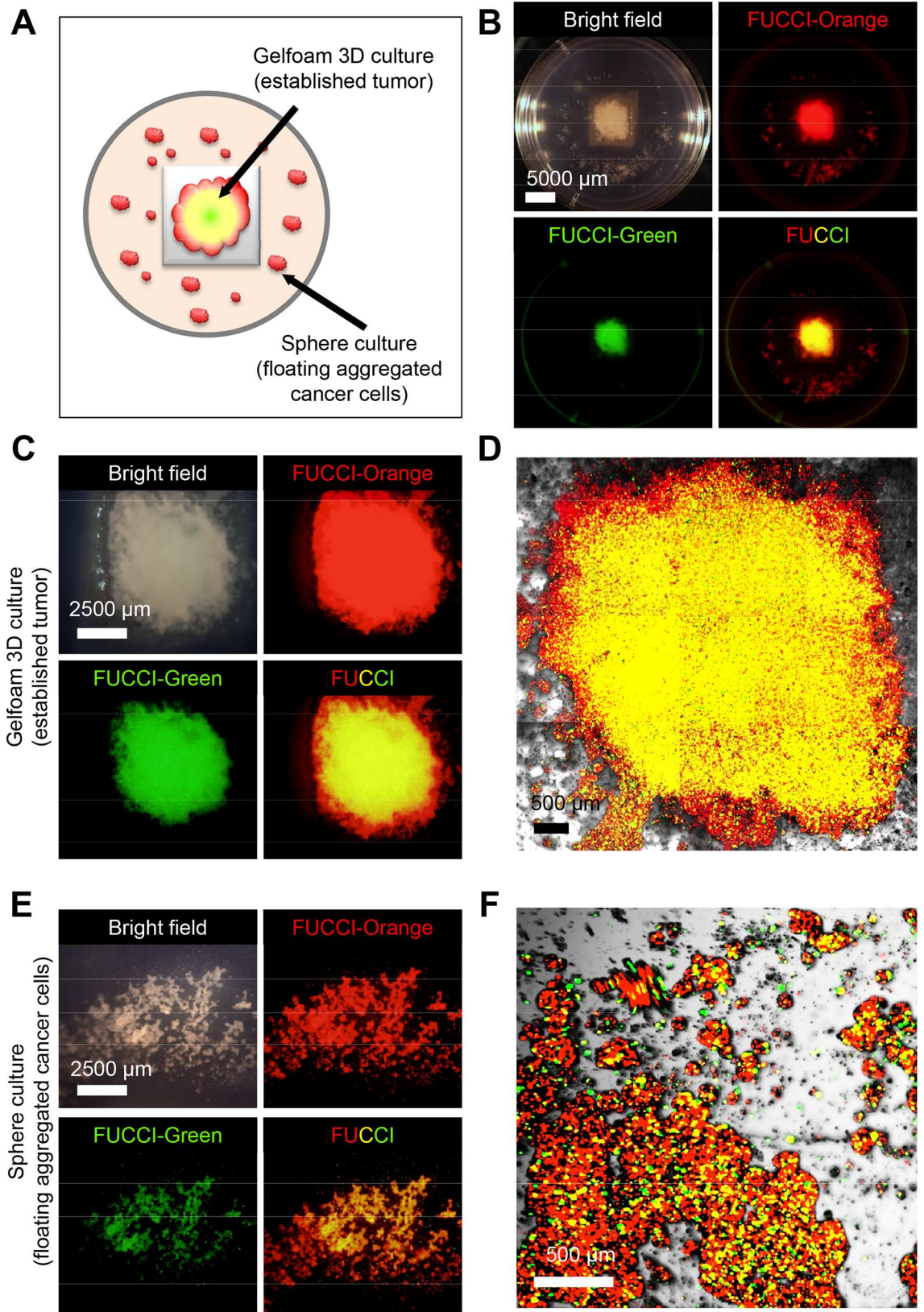


Fig 2. Cell cycle distribution of MKN-45 cells forming tumors on Gelfoam[®]. Sterile Gelfoam[®] sponges (Pharmacia & Upjohn, Kalamazoo, MI), prepared from porcine skin, were cut into 1 cm cubes. The Gelfoam[®] cubes were incubated at 37°C in order that Gelfoam[®] absorbed the RPMI 1640 medium. The absorbed Gelfoam[®] was placed on agarose in 35 mm dishes. FUCCI-expressing MKN-45 cells were seeded on the absorbed Gelfoam[®] for 3D culture. MKN-45 cells formed tumor-like structures on Gelfoam[®] and spheres on the agarose. **A.** Schema of Gelfoam[®] cultures on agarose. **B.** Macroscopic appearance of MKN-45 cancer cells forming tumor-like structures on Gelfoam[®]. Images were acquired with the OV100 variable magnification fluorescence imager (Olympus, Japan). **C.** Macroscopic appearance of MKN-45 tumor-like structures growing on Gelfoam[®]. Images were acquired with the OV100. **D.** Representative images of the MKN-45 tumor-like structure on Gelfoam[®] using the FV1000 confocal laser scanning microscope (Olympus). **E.** Macroscopic images of MKN-45 spheres growing in agar. **F.** Microscopic FUCCI image of MKN-45 spheres.

doi:10.1371/journal.pone.0162991.g002

periods of time and sorted for the fluorescence color corresponding to plasmid used as described previously in detail [12].

Imaging of FUCCI-Expressing MKN-45 Cells

The OV100 variable magnification fluorescence imaging system (Olympus) was used to acquire macro images as described previously in detail [20]. The FV1000 confocal laser scanning microscope (Olympus) was used to image single FUCCI-expressing cells. The FV1000 contains 473 nm and 559 nm lasers [21]. The 4× objective lens with a 0.20 numerical aperture and the 20× objective lens with a 0.95 numerical aperture were used. Fluoview software (Olympus) was used for image acquisition and Velocity 6.0 version (Perkin Elmer) [15] were used for 3D analysis. The above methods were previously described in detail [21].

Statistical Analysis

The Student's *t*-test was used for comparison of 2 groups. Data are presented as means ± SD. Significance was determined via a *P* value of < 0.05 [12].

Results and Discussion

Cell-cycle Decoy and Killer Efficacy of Telomerase-Dependent Adenovirus OBP-301 in Comparison with Chemotherapy on Tumor Spheres

FUCCI-expressing MKN-45 stomach cancer cells cultured on agarose spontaneously formed spheres and were mostly FUCCI red, indicating they were in G₀/G₁ phase (Fig 1A). Tumor spheres were treated with OBP-301, cisplatin (CDDP), or paclitaxel (Fig 1B). CDDP- or paclitaxel-treated MKN-45 cells remained in the quiescent G₀/G₁ state and did not change size compared with control-spheres or spheres before treatment (Fig 1C–1E). In contrast, OBP-301 decoyed the cell cycle of tumor spheres from G₀/G₁ phase to S/G₂ phase where they expressed FUCCI green and reduced the size of the tumor (Fig 1C–1E). G₀/G₁ cancer cells in spheres were resistant to chemotherapy but could be decoyed to S/G₂ by OBP-301 which reduced their viability.

Cell-cycle Distribution of MKN-45 Stomach Cancer Cells Forming Tumors on Gelfoam[®]

FUCCI-expressing MKN-45 cells on Gelfoam[®] grew into tumor-like structures with the majority of the cells in G₀/G₁ (Fig 2) when the tumor-like structure matured. The mature tumors or spheres on Gelfoam[®] have the vast majority of their cells in G₀/G₁ (Figs 1E and 3E and 3F) and thereby look red or yellow. The images are of the whole tumor or sphere, not cross

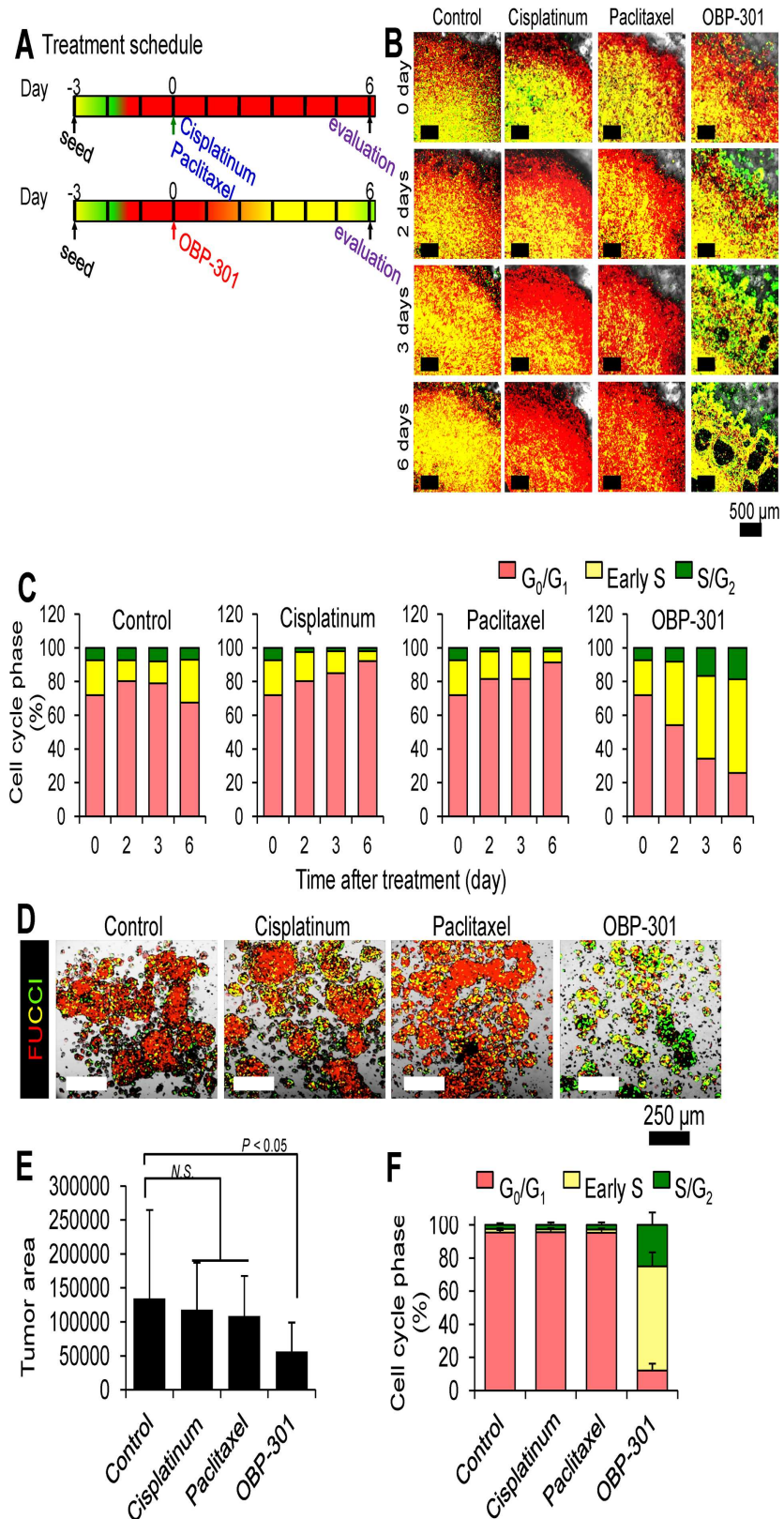


Fig 3. Time-course imaging of decoy of quiescent MKN-45 cancer cells in tumor-like structures on Gelfoam[®] by OBP-301 and their subsequent killing. A. Experimental setup for treatment of MKN-45

tumor-like structures growing in Gelfoam[®] with OBP-301, CDDP, or paclitaxel. **B.** Time-course images of FUCCI-expressing MKN-45 cancer cells forming tumor-like structures on Gelfoam[®] treated with OBP-301, CDDP, or paclitaxel. The cells in G₀/G₁, S, or G₂/M phases appear red, yellow, or green fluorescent, respectively. **C.** Histogram shows the cell cycle phase of FUCCI-expressing MKN-45 cancer cells forming tumor-like structures on Gelfoam[®] treated with OBP-301, CDDP, or paclitaxel. **D.** Representative images of control, OBP-301-, CDDP-, or paclitaxel-treated tumors. **E.** Bar graphs show the size of viable tumor after each treatment. **F.** Histogram shows cell-cycle phase of MKM-45 cells in treated and untreated spheres. Scale bars, 100 μm. Data are shown as means ± SD (n = 5). *P < 0.01. The percentage of cells in G₀/G₁, S, and G₂/M phases are shown.

doi:10.1371/journal.pone.0162991.g003

sections. The yellow fluorescence is derived from the mixture of red (G₀/G₁) and green (cycling) cells on the surface of the sphere or tumor on Gelfoam[®].

OBP-301 Decoyed Quiescent Cancer Cells in Tumors Growing on Gelfoam[®] to Cycle and Reduced Their Viability

Gelfoam[®] histocultures of FUCCI-expressing MKN-45 cancer cells were treated with OBP-301, CDDP, or paclitaxel (Fig 3A). Only cycling MKN-45-FUCCI cells were sensitive to CDDP and paclitaxel; quiescent G₀/G₁ MKN-45 cells were resistant to these drugs (Fig 3B). In contrast, OBP-301 decoyed the MKN-45 cells in the tumor-like structures on Gelfoam[®] to cycle from G₀/G₁ phase to S/G₂ phase and reduced their viability (Fig 3B and 3C). CDDP- or paclitaxel-treated MKN-45 tumor-like structure remained quiescent and did not change in size (Fig 3D and 3E). In contrast, OBP-301 reduced the size of the MKN-45 tumor-like structures on Gelfoam[®] (Fig 3D–3F).

OBP-301 Modulates Cell-Cycle Related Gene Expression

We examined the cell cycle-related proteins using Western blotting. CDDP increased the expression of p53 and p21 indicating cell-cycle arrest. In contrast, OBP-301 decreased the expression of p53 and p21 (Fig 4). Furthermore, OBP-301 increased the expression of E2F and pAkt indicating in cell-cycle decoy (Fig 4).

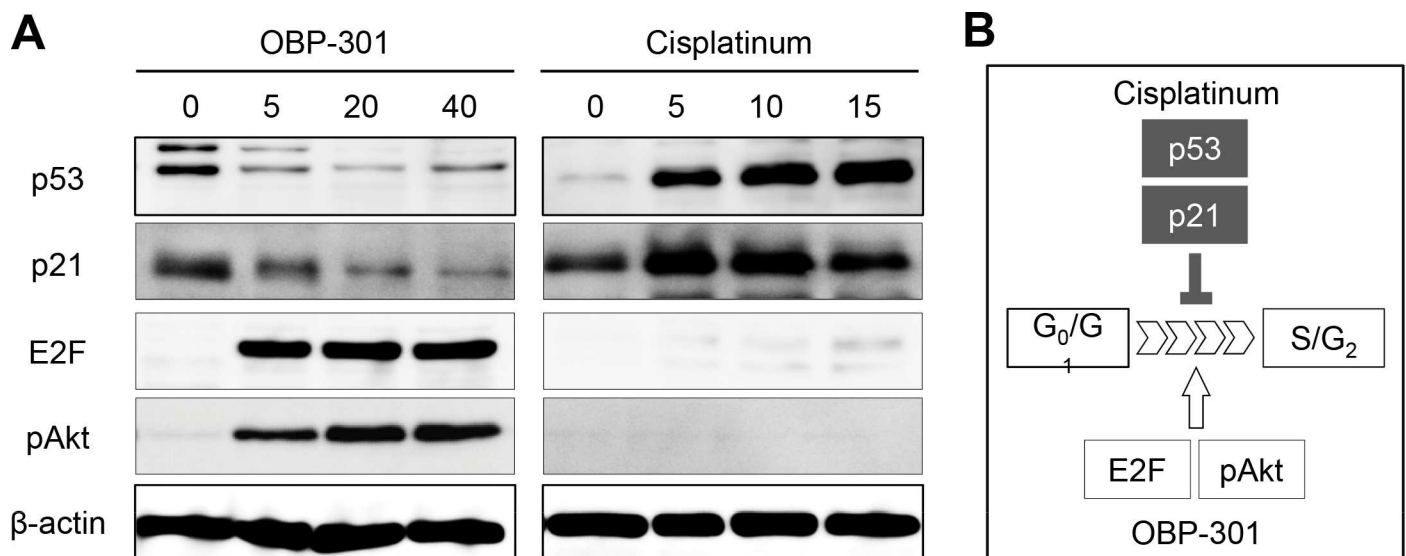


Fig 4. A. Western blots show the expressions of p53, p21, E2F, and pAkt after OBP-301 or CDDP treatment. **B.** The scheme of cell cycle change.

doi:10.1371/journal.pone.0162991.g004

The cell cycle decoy effect of OBP-301 is large scale, whereby the cells in untreated mature spheres or Gelfoam[®] tumor are almost all in G₀/G₁ and almost all of them cycle after OBP-301 infection. The sphere or tumor area is reduced by approximately one half after OBP-301 treatment which is not as great an effect as the extent of decoy. Future experiments will investigate the kinetics of cancer-cell killing after OBP-301 treatment.

Conclusions

SCCP growing as spheres or tumor-like structures on Gelfoam[®] cycle became mostly quiescent as they matured and were thereby resistant to chemotherapy. Telomerase-dependent adenovirus OBP-301 could decoy the quiescent tumor cells in spheres or tumor-like structures in Gelfoam[®] to begin to cycle whereby they lost viability. These results are further demonstration of the power of cell-decoy chemotherapy.

Acknowledgments

This paper is dedicated to the memory of A.R. Moossa, M.D.

Author Contributions

Conceptualization: SY RMH.

Data curation: SY RMH.

Formal analysis: SY KT RMH.

Funding acquisition: TF RMH.

Investigation: SY KT RMH.

Methodology: SY KT RMH.

Project administration: RMH.

Resources: HT HK YU SK TF RMH.

Supervision: TF RMH.

Validation: SY RMH.

Visualization: SY KT RMH.

Writing – original draft: SY RMH.

Writing – review & editing: SY RMH.

References

1. Leighton J. (1954) The growth patterns of some transplantable animal tumors in sponge matrix tissue culture. *J Natl Cancer Inst* 15:275–293. PMID: [13233883](#)
2. Tome Y, Uehara F, Mii S, Yano S, Zhang L, Sugimoto N, et al. (2014) 3-dimensional tissue is formed from cancer cells in vitro on Gelfoam[®], but not on Matrigel[™]. *J Cell Biochem* 115:1362–1367. doi: [10.1002/jcb.24780](#) PMID: [24497277](#)
3. Hoffman RM. Application of GFP imaging in cancer. *Laboratory Investigation* 95, 432–452, 2015. doi: [10.1038/labinvest.2014.154](#) PMID: [25686095](#)
4. Freeman AE, Hoffman RM. (1986) In vivo-like growth of human tumors in vitro. *Proc Natl Acad Sci USA* 83:2694–2698. PMID: [3458228](#)
5. Hoffman RM. (2013) Tissue Culture. In: *Brenner's Encyclopedia of Genetics*, 2nd Ed., 7:73–76.

6. Mii S, Duong J, Tome Y, Uchugonova A, Liu F, Amoh Y, et al. (2013) The role of hair follicle nestin-expressing stem cells during whisker sensory-nerve growth in long-term 3D culture. *J Cell Biochem* 114:1674–1684. doi: [10.1002/jcb.24509](https://doi.org/10.1002/jcb.24509) PMID: [23444061](https://pubmed.ncbi.nlm.nih.gov/23444061/)
7. Mii S, Uehara F, Yano S, Tran B, Miwa S, Hiroshima Y, et al. (2013) Nestin-expressing stem cells promote nerve growth in long-term 3-dimensional Gelfoam[®]-supported histoculture. *PLoS One* 8: e67153. doi: [10.1371/journal.pone.0067153](https://doi.org/10.1371/journal.pone.0067153) PMID: [23840607](https://pubmed.ncbi.nlm.nih.gov/23840607/)
8. Mii S, Amoh Y, Katsuoka K, Hoffman RM. (2014) Comparison of nestin-expressing multipotent stem cells in the tongue fungiform papilla and vibrissa hair follicle. *J Cell Biochem* 115:1070–1076. doi: [10.1002/jcb.24696](https://doi.org/10.1002/jcb.24696) PMID: [24142339](https://pubmed.ncbi.nlm.nih.gov/24142339/)
9. Duong J, Mii S, Uchugonova A, Liu F, Moossa AR, Hoffman RM. (2012) Real-time confocal imaging of trafficking of nestin-expressing multipotent stem cells in mouse whiskers in long-term 3-D histoculture. *In Vitro Cell Dev Biol Anim* 48:301–305. doi: [10.1007/s11626-012-9514-z](https://doi.org/10.1007/s11626-012-9514-z) PMID: [22580909](https://pubmed.ncbi.nlm.nih.gov/22580909/)
10. Li L, Margolis LB, Paus R, Hoffman RM. (1992) Hair shaft elongation, follicle growth, and spontaneous regression in long-term, gelatin sponge-supported histoculture of human scalp skin. *Proc Natl Acad Sci USA* 89:8764–8768. PMID: [1528891](https://pubmed.ncbi.nlm.nih.gov/1528891/)
11. Grivel JC, Ito Y, Fagà G, Santoro F, Shaheen F, Malnati MS, et al. (2001) Suppression of CCR5- but not CXCR4-tropic HIV-1 in lymphoid tissue by human herpesvirus 6. *Nat Med* 7:1232–1235. PMID: [11689888](https://pubmed.ncbi.nlm.nih.gov/11689888/)
12. Yano S, Miwa S, Mii S, Hiroshima Y, Uehara F, Yamamoto M, et al. (2014) Invading cancer cells are predominantly in G₀/G₁ resulting in chemoresistance demonstrated by real-time FUCCI imaging. *Cell Cycle* 13:953–960. doi: [10.4161/cc.27818](https://doi.org/10.4161/cc.27818) PMID: [24552821](https://pubmed.ncbi.nlm.nih.gov/24552821/)
13. Hoffman RM. (2015) Application of GFP imaging in cancer. *Laboratory Investigation* 95:432–452. doi: [10.1038/labinvest.2014.154](https://doi.org/10.1038/labinvest.2014.154) PMID: [25686095](https://pubmed.ncbi.nlm.nih.gov/25686095/)
14. Yano S, Miwa S, Mii S, Hiroshima Y, Uehara F, Kishimoto H, et al. (2015) Cancer cells mimic in vivo spatial-temporal cell-cycle phase distribution and chemosensitivity in 3-dimensional Gelfoam[®] histoculture but not 2-dimensional culture as visualized with real-time FUCCI imaging. *Cell Cycle* 14:808–819. doi: [10.1080/15384101.2014.1000685](https://doi.org/10.1080/15384101.2014.1000685) PMID: [25564963](https://pubmed.ncbi.nlm.nih.gov/25564963/)
15. Yano S, Zhang Y, Miwa S, Tome Y, Hiroshima Y, Uehara F, et al. (2014) Spatial-temporal FUCCI imaging of each cell in a tumor demonstrates locational dependence of cell cycle dynamics and chemoresponsiveness. *Cell Cycle* 13:2110–2119. doi: [10.4161/cc.29156](https://doi.org/10.4161/cc.29156) PMID: [24811200](https://pubmed.ncbi.nlm.nih.gov/24811200/)
16. Yano S, Tazawa H, Hashimoto Y, Shirakawa Y, Kuroda S, Nishizaki M, et al. (2013) A genetically engineered oncolytic adenovirus decoys and lethally traps quiescent cancer stem-like cells into S/G₂/M phases. *Clin. Cancer Res* 19:6495–6505. doi: [10.1158/1078-0432.CCR-13-0742](https://doi.org/10.1158/1078-0432.CCR-13-0742) PMID: [24081978](https://pubmed.ncbi.nlm.nih.gov/24081978/)
17. Yokozaki H. Molecular characteristics of eight gastric cancer cell lines established in Japan. *Pathol Int* 2000; 50:767–77. PMID: [11107048](https://pubmed.ncbi.nlm.nih.gov/11107048/)
18. Hoffman RM. Histocultures and their use. In: *Encyclopedia of life sciences*. Chichester: John Wiley and Sons Ltd. Published Online. 2010; doi: [10.1002/9780470015902.a0002573.pub2](https://doi.org/10.1002/9780470015902.a0002573.pub2)
19. Sakaue-Sawano A, Kurokawa H, Morimura T, Hanyu A, Hama H, Osawa H, et al. (2008). Visualizing spatiotemporal dynamics of multicellular cell cycle progression. *Cell* 132:487–498. doi: [10.1016/j.cell.2007.12.033](https://doi.org/10.1016/j.cell.2007.12.033) PMID: [18267078](https://pubmed.ncbi.nlm.nih.gov/18267078/)
20. Yamauchi K, Yang M, Jiang P, Xu M, Yamamoto N, Tsuchiya H, et al. (2006) Development of real-time subcellular dynamic multicolor imaging of cancer-cell trafficking in live mice with a variable-magnification whole-mouse imaging system. *Cancer Res* 66:4208–4214. PMID: [16618743](https://pubmed.ncbi.nlm.nih.gov/16618743/)
21. Uchugonova A, Duong J, Zhang N, König K, Hoffman RM. (2011) The bulge area is the origin of nestin-expressing pluripotent stem cells of the hair follicle. *J Cell Biochem* 112:2046–2050. doi: [10.1002/jcb.23122](https://doi.org/10.1002/jcb.23122) PMID: [21465525](https://pubmed.ncbi.nlm.nih.gov/21465525/)